Kybernetik 12, 74—89 (1973)

Development and Application of White-Noise Modeling Techniques for Studies of Insect Visual Nervous System

P. Z. Marmarelis and G. D. McCann
California Institute of Technology Pasadena, California, USA

Received: August 3, 1972

Abstract

The nonlinear system identification technique through white-noise stimulation is extended to multi-input, -output systems with consideration given to applications in the functional study of the nervous system. The applicability of the method is discussed in general and in particular for the motion detection neuronal system of the fly. Two series of experiments are performed; one with moving striped-pattern stimuli and the other with spot stimuli of fluctuating intensity. In both cases nonlinear dynamic models are derived which describe the system with considerable accuracy over the frequency range of 0.2–50 Hz and a dynamic amplitude range of about 40–1. These models are able to predict accurately all the discrete experiments so far performed on this system for which the models are applicable. The differences in dynamic characteristics between the corresponding system of the *Musca* and *Phaenicia* families of flies are minor except for a difference in latencies and if the difference in geometry of their faceted eyes is taken into account. The large field response of the motion detection unit is a linear weighted summation of all the smaller field highly nonlinear subsystems of which the large field is comprised.

I. Introduction

Research on visual nervous systems at the detailed neural network level has reached the stage where the formidable problems of determining complex functional interactions between the different neural subsystems are becoming clearly apparent. These subsystems, in processing visual information, may demonstrate widely varied and complex properties with respect to such general visual parameters as intensity, color, form, motion and binocular depth of perception. The design and execution of the many required suitable individual experiments to ferret out accurately these pertinent system properties is a long and tedious process.

The potential capability of nonlinear identification theory through white-noise stimulation (Marmarelis, 1972) to obtain a wide range of response properties in a concise mathematical description from one "universal" experiment is therefore intriguing. There are, however, some important difficulties that must be adequately assessed in order to use it properly, such as the fact that the theory presumes stationarity of both the signal and noise. The range of temporal frequencies, intensities and other parametric variations can be quite large and the accuracy required in the experimental data and the computational procedures for determining the characterizing system functionals increases rapidly with the range of such variations. Several serious efforts have been made to use this theory in vertebrate eye research (Marmarelis and Naka, 1972; Marmarelis, 1971). However, these have been confined to systems whose inputs are spatially stationary stimuli which are functions of one independent variable (time). Since one or more spatial variables are also of great importance in the visual system, the theory and experimental techniques are extended to apply to these additional cases. Basic studies have shown this to be feasible and a logical first step to such extensions is illustrated here.

Summary Description of Systems Studied. The system chosen for this study is a group of selective motion detection fibers of flies, all of which combine the same basic small field selective motion detection processes along two coordinate directions relative to the head (approximately horizontally and vertically) (McCann and Dill, 1969). This system was chosen for this study because its response properties had already been studied in considerable detail. A preliminary series of discrete experiments provide the principal basis for evaluating the parameters of the white-noise tests (McCann). The motion detection process can be studied by microelectrode recordings from four levels of neuronal units. The first of these have elliptical fields of about 15 degrees across the major axis. The fourth level possesses the full field of one eye represented by a horizontal angular spread of about 200 degrees and a vertical spread of 360 degrees (Bishop *et al.*, 1968).

Tests with small spot stimuli (McCann) have produced approximate algorithms for the small field processes in the two horizontal and vertical directions. Rows of small field units with lateral inhibition are indicated as contributing to the basic motion detection processes which are correlations between adjacent pairs of these units (McCann). The visual fields of the horizontal set of form units and of the correlation process are shown in Fig. 1. It has been shown that the full eye field motion detection fibers for each coordinate (called Class II units) combine the small field unit motion detection reaction as a rather simple algebraic summation with no interaction between the horizontal and vertical systems (McCann and Foster, 1971). The system of retinular cells, the small field form units and the four levels of selective motion detection units can all be studied experimentally. This initial study has undertaken the direct determination of the mathematical descriptions of both the basic small field motion detection processes and the full field response properties of the Class II units through white-noise visual stimuli and the evoked responses of the Class II units.

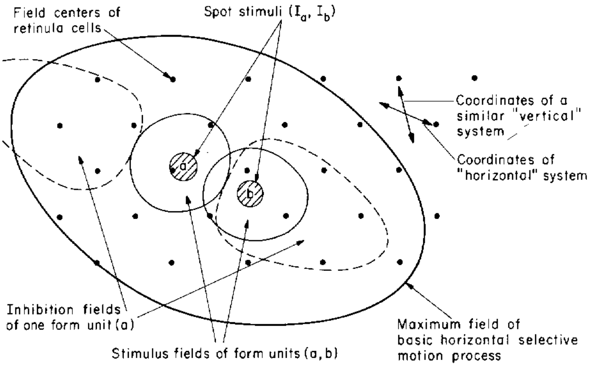

Fig. 1. Geometrical relations between field centers of retinula cells, the stimulus and inhibition fields of the "form" units (Arnett) and the basic motion field over which two spot correlation is made for motion detection. Also shown are the two spot stimuli (I_a, I_b)

Design of the White-Noise Identifying Experiments. Consideration will first be given to the possibility of designing a suitable stimulus to determine the complete functional processes of a full field selective motion detection unit (Class II) as defined by a nonlinear dynamic transfer response function between visual stimulus and the unit response. This must be a stimulus that covers the complete temporal frequency, spatial frequency and intensity response ranges. The energy distribution must be equally distributed over intensity and randomly distributed relative to the temporal and spatial frequencies. As a first simplification let it be assumed that only a one-dimensional space variable pattern is designed to test only the horizontal directions of motion detection.

This system has long time constant (6 min.) adaptation properties. One of these (until recently found only in higher order vertebrates) optimizes the detection threshold of patterns when the pattern background illumination is equal to the adaptation level (McCann and Foster, 1972). Thus the complete temporal frequency range of the responses is from about 0.003 Hz to the 50 Hz found for the upper limit from the spot stimulus studies (McCann). The acuity of the system permits the detection of spatial frequencies below about three degrees. Thus the pattern would have to cover a solid angle of 200 degrees with a random distribution of spatial wavelengths between 3 and 200 degrees. Finally, the test pattern would have to cover an intensity range of over 1000–1 (McCann and MacGinitie, 1965).

Stimulus patterns of this character and with very good signal-to-noise ratios are feasible with modern cathode-ray display techniques. One of the prime considerations, however, is the fact that a stimulus with such a broad range of properties has a small probability of diclosing great detail in any one narrow band of the range. Additional complications are presented by noise in the response recordings. The required duration of a white-noise stimulus in order to obtain a given accuracy in the derived model depends on the following: the signal-to-noise ratio; the number of response points recorded per unit time and the bandwidth of the temporal frequency; the spatial frequency and intensity ranges. Neuronal recordings producing continuously varying potentials require shorter duration tests than time-of-event recordings of spikes such as chosen here.

Tests described below showed that in the case of time-of-event recordings from the Class II units a white-noise stimulus presenting temporal variations from only 0.2–50 Hz with 1.6 log units of intensity range required an experimental length of 400 seconds (10 experiments of 40 sec each) to obtain satisfactory accuracy. Thus, if just the range of temporal frequencies was extended to the 0.003–50 Hz given above the required duration would be raised to about 6.5 hours. A final limitation is the required computing time to calculate the characterizing kernels of the series expression for the functions. This would be astronomical for such a long stimulus. The complete coverage of temporal, spatial and intensity parameters in one stimulus is thus clearly impractical.

Since the two-spot tests illustrated by Fig. 1 gave so much functional detail it was decided to choose a similar pair of white-noise stimuli as the first of a group of comprehensive tests to determine the properties of the motion detection functions. This should have the capability of verifying and adding to the several hundred individual tests made with discrete spots (McCann). The second type of stimulus was one in which a large striped pattern was presented with white-noise motion along the horizontal coordinate of motion detection. It will be shown below that if large field motion detection is a linear weighted algebraic summation of small field nonlinear motion detection responses, a simple relationship must exist between the functions representing them. Therefore, the two series of tests would verify or disprove the laws of both basic small field and large field motion detection.

II. White Noise Stimulation Theory for Single and Multi-Input, -Output Systems

The problem of identification of systems is concerned with determining the input-output transfer characteristics of the system; that is, the determination of the system functional F, ($y(t)=F[x(t)]$), where $x(t)$ is the system input and $y(t)$ is the system output.

Two different goals of the identification process can be distinguished; one could be called "functional identification" and corresponds to finding *what F is* and the other could be called "structural identification" and corresponds to finding *how F is computed* by the physical system. The second goal presupposes some *a priori* information about the system's internal structure and it usually takes the form of estimating certain parameters of the system. The first goal treats the system or parts of it as a black box and is, therefore, a more primitive process in the whole modeling procedure. The following provides a definition of the identification problem: *Given* a system $y(t)=F[x(t)]$ choose a set of stimuli $\{x_i\}$ such that the stimulus-response pairs $\{x_i, y_i\}$ obtained experimentally will allow the determination of F. The solution of the problem is in terms of a derived mathematical model which allows the prediction of the system behaviour for a very wide class of input functions.

Single-Input, -Output System. As has been described elsewhere (Marmarelis, 1971), the system model (transfer functional) is in terms of a Volterra series,

$$y(t)=h_0+\int_0^\infty h_1(\tau)\,x(t-\tau)\,d\tau + \iint_0^\infty h_2(\tau_1,\tau_2)\,x(t-\tau_1)\,x(t-\tau_2)\,d\tau_1\,d\tau_2+\cdots \tag{1}$$

whose set of kernels $\{h_0, h_1, h_2, \ldots\}$ are obtained by subjecting the system to white-noise stimulation. This set of kernels completely characterizes the system and it can be interpreted to reveal certain functional traits of it.

The method is based on Wiener's idea that a nonlinear system can be identified by its response to Gaussian white-noise since, with such a stimulus, the system will effectively be tested with all possible inputs (Wiener, 1958). The class of systems that are time-invariant and have a finite memory can be analyzed by this method. Wiener (1958) showed that two systems are equivalent if their responses to white-noise are identical. Therefore, it is proposed that the performance of a model of a nonlinear system is measured by comparing its response to white-noise with the response of the physical system to this same input.

In the first series of experiments the stimulus is a moving pattern of stripes whose displacement from the rest position varies in time in white-noise fashion. From this identifying experiment a model is derived which can predict the response of the Class II unit to any motion of this pattern of stripes. The functional equation relating the position of the stripes, $s(t)$, to the response $r(t)$ of the unit is given by

$$r(t)=h_0+\int_0^\infty h_1(\tau)\,s(t-\tau)\,d\tau + \iint_0^\infty h_2(\tau_1,\tau_2)\,s(t-\tau_1)\,s(t-\tau_2)\,d\tau_1\,d\tau_2 \tag{2}$$

where the functions $h_0, h_1(\tau)$, $h_2(\tau_1,\tau_2)$ have been computed from the characterizing white-noise experiment. Term h_0 is just the average response of the unit while $h_1(\tau)$ and $h_2(\tau_1,\tau_2)$ are the linear and nonlinear system kernels and are shown in Fig. 2 and Table I. Using Eq. (2) and the kernels of Fig. 2 and Table I, one can compute the response of the Class II unit to any moving sequence of the striped pattern.

Extension to Multi-Input, -Output Systems: the theory has been extended to include multi-input, -output systems. Consider, for example, a system with two inputs, $I_a(t)$ and $I_b(t)$ and one output $R(t)$. Then it can be shown that

$$R(t)=\sum_{n=0}^{\infty} G_n[\{h\}_n, I_a(t), I_b(t)] \tag{3}$$

where $\{h\}_n$ is a set of kernels of degree n and $I_a(t)$, $I_b(t)$ are two independent gaussian white-noise signals.

The terms of this series are given by

$$\begin{aligned}
&G_0[\{h\}_0, I_a(t), I_b(t)] = h_0\\
&G_1[\{h\}_1, I_a(t), I_b(t)]\\
&\quad = \int_0^\infty h_{1a}(\tau)\, I_a(t-\tau)\, d\tau + \int_0^\infty h_{1b}(\tau)\, I_b(t-\tau)\, d\tau\\
&G_2[\{h\}_2, I_a(t), I_b(t)]\\
&\quad = \iint_0^\infty h_{2aa}(\tau_1,\tau_2)\, I_a(t-\tau_1)\, I_a(t-\tau_2)\, d\tau_1\, d\tau_2\\
&\qquad - P_a \int_0^\infty h_{2aa}(\tau,\tau)\, d\tau\\
&\qquad + \iint_0^\infty h_{2bb}(\tau_1,\tau_2)\, I_b(t-\tau_1)\, I_b(t-\tau_2)\, d\tau_1\, d\tau_2\\
&\qquad - P_b \int_0^\infty h_{2bb}(\tau,\tau)\, d\tau\\
&\qquad + \iint_0^\infty h_{2ab}(\tau_1,\tau_2)\, I_a(t-\tau_1)\, I_b(t-\tau_2)\, d\tau_1\, d\tau_2
\end{aligned} \tag{4}$$

where P_a is the power level of white-noise input $I_a(t)$ (i.e. $\Phi_{xx}(f) = P_a$) and P_b is the power level of input $I_b(t)$. Kernels $h_{2aa}(\tau_1, \tau_2)$ and $h_{2bb}(\tau_1, \tau_2)$ are symmetric functions of their arguments. Kernel $h_{2ab}(\tau_1, \tau_2)$ is, in general, an asymetric function of its arguments and it describes the nonlinear interaction between the two inputs $I_a(t)$ and $I_b(t)$. Kernel h_{2ab} will be referred to as the cross-kernel and h_{1a}, h_{2aa}, h_{1b}, h_{2bb} as the self-kernels. These kernels are given by,

$$\begin{aligned}
h_{1a}(\sigma) &= (1/P_a)\, E\{R(t)\, I_a(t-\sigma)\}\\
h_{1b}(\sigma) &= (1/P_b)\, E\{R(t)\, I_b(t-\sigma)\}\\
h_{2aa}(\sigma_1,\sigma_2) &= (1/2\, P_a^2)\, E\{R(t)\, I_a(t-\sigma_1)\, I_a(t-\sigma_2)\}\\
h_{2bb}(\sigma_1,\sigma_2) &= (1/2\, P_b^2)\, E\{R(t)\, I_b(t-\sigma_1)\, I_b(t-\sigma_2)\}\\
h_{2ab}(\sigma_1,\sigma_2) &= (1/2\, P_a P_b)\, E\{R(t)\, I_a(t-\sigma_1)\, I_b(t-\sigma_2)\}
\end{aligned} \tag{5}$$

where $E\{Z\}$ denotes the expected value of Z. If higher order kernels are required they can be computed following similar procedures. This extension to multi-input systems is based on the cross-correlation techniques of Lee and Schetzen (1961).

There are several considerations to be made in planning the identifying experiment in order to minimize the effort required to achieve a certain accuracy. These have been described in detail elsewhere (Marmarelis, 1972) and are summarized here.

The conditions for the time-invariancy of the system must be established. The amplitude range and frequency bandwidth of the stimulus must be chosen to cover the operational range of the system (amplitude-wise and frequency-wise). It has been shown, however, that if the noise bandwidth extends too much beyond the system bandwidth then the error in the kernel estimates is large.

Since the n-th order term of the series can produce at most an n-th order harmonic in the response, a preliminary harmonic analysis of the response to sinusoidal stimuli determines the dominant terms in the series that must be computed in order to achieve a certain accuracy.

The memory of the system must be measured in order to determine the extent to which the kernels must be computed and the temporal length of the characterizing experiment. The bandwidth of the system should be measured from a preliminary computation of the response power spectrum so as to determine the white-noise bandwidth. The length of the characterizing experiment for a certain statistical variance in the kernel estimates can be calculated from the system memory and the white-noise stimulus bandwidth.

Analysis of the error introduced by additive noise at the input, output or internally has shown that errors at the input are much more serious than errors at the output (Marmarelis, 1972). They tend to increase with both the order of nonlinearity of the system and the order of the computed kernel. These error terms are given as convolutions of the system kernels with the correlation functions of the noise with the signal. It is shown that, in many cases, if the noise is independent of the signal then the kernel estimate is unaffected by the presence of this noise. This is an important advantage of this method in determining the characterizing kernels. In view of the above it is essential to produce accurate white-noise stimuli.

It has been shown that computation time for the n-th order kernel increases almost exponentially with the order of the kernel, thus severely limiting the extent to which the series of Eq. (1) can be computed by conventional means. The terms of Eq. (1) can be in a form such that they are mutually orthogonal (Wiener, 1958). Each term of a certain degree is computed in this orthogonal form before it is put in the form of Eq. (1). Therefore, the addition of the n-th term produces a model of n-th degree with optimum performance in the mean-square-error sense without necessitating the recomputation of the previously determined terms.

III. Experimental Methods

The extracellular microprobing techniques for recording the Class II units have been described elsewhere (McCann and Dill, 1969). The most important new consideration is the generation and recording of accurate white-noise stimuli and the acquisition of response data with satisfactoily high signal-to-noise ratios. Different techniques were used for the two types of stimuli. The large moving stimulus was a 40 degree diameter circular striped pattern with a spatial wavelength of 10 degrees. It was projected from an incandescent source onto a reflecting screen via a moving mirror whose angular motion was controlled by a white-noise current signal into an electromagnetic transducer. The projected pattern motion (i.e. displacement of stripes from their rest position as a function of time) was within one percent of the white-noise values generated digitally which had a temporal frequency bandwidth from d.c. to 50 Hz. The response phase shift was less than 2 degrees over this range. The amplitude range of the motion was varied in different experiments from 0.5–8 degrees since a variation of this parameter provided information on the effective sampling station spacing for the small field motion correlation process.

Illumination for the two spot stimuli was provided by Sylvania R 1131 C glow modulator tubes whose spectral response properties vary only slightly over a 70–1 intensity range. To show that this variation had no effect in the Class II unit responses, whose signals are derived primarily from one class of retinula cells (McCann and Arnett, 1972), tests were made both with and without a broad band green filter that suppressed the variable portion of the stimulus spectrum. Moreover, as the small variation in the spectral composition of the stimulus occurs only at very low intensity levels which occupy the low-probability tail of the gaussian distribution in the stimulus signal, the derived characterizations were unaffected because of the used cross-correlation technique by which the characterizing kernels are computed (Marmarelis, 1972).

Digital-to-analog convertors were used to convert white-noise signals generated in digital form to the direct analog control signals for both types of stimuli. Separate uncorrelated white-noise signals were used for the two spots. The spot size ranged from one half degree diameter circles to a pair of vertical bars one half degree in the direction of motion detection and five degrees high. The mean intensity of the two spots was set half way between the threshold and response saturation intensities of the Class II units. This had approximately a 50–1 range and the intensity was then varied plus and minus over this range. The frequency spectra of the white-noise representations provided by both types of stimuli are shown in Fig. 4 and Fig. 7.

Data Processing. The data processing scheme involved generation and control of the white-noise stimulus by a small computer (SCC 4700) and interaction with a central computer (IBM 360/44) through an IBM 2250 display terminal. This interaction included on-line display and preliminary analysis of the stimulus and response records such as auto- and cross-correlations and histogramming. For example, at this stage the signal-to-noise ratios were estimated by correlating the responses to identical runs of white-noise stimuli which in turn determined the smoothing function of the response waveform. The following procedure was followed in order to convert the spike records into continuous functions of time: The white-noise stimulus record was formed by concatenating several (6–12) identical (40 second duration) white-noise records. The unit responses to these runs of identical white-noise were superimposed and histogrammed in time to produce a continuous function which denotes the spike frequency as a function of time. Such a procedure resulted in a waveform with some artificially introduced high frequencies which were subsequently filtered out (smoothing) through the use of an appropriate smoothing window. The smoothing window was determined by the measured cross-correlogram of responses to identical white-noise stimuli (Fig. 5a). The width of the peak of the correlogram indicates the extent of "jitter" in the triggering of the spikes and therefore represents some form of high-frequency noise. The smoothing window is designed to fit the form of the measured correlogram.

The stimulus-response data were then treated for reduction of long-term drifts. This was accomplished through subtracting an appropriate mean square curve from the response record, such as linear, parabolic and exponential trends. In this way the zeroth order kernel, h_0, was set equal to zero in Eq. (1). Whenever needed in the analysis the mean response level was taken to be the constant term of these fitted curves. The exact value of the power level of the input, P, (also P_a, P_b in the case of two-input systems) is picked by use of a variational technique which minimizes the mean square error between model and experimental responses to the same white-noise input over the entire length of the identifying experiment. The computation of the power spectra was done taking into account many of the subtleties and difficulties of this procedure (Marmarelis, 1971).

IV. Experimental Results and Derived Models

Moving Patterns. In this series of experiments a moving striped pattern (described earlier) was used as the stimulus and the evoked response was recorded from a Class II selective motion detection unit. The stripes were moved about their resting position in white-noise fashion while the pattern boundaries remained stationary. The distribution of the excursions (amplitudes measured from mid-position) was a gaussian truncated at about 2.5 standard deviations. It has been shown (Marmarelis, 1972) that this truncated introduces negligible error in the kernel estimates.

Since selective motion detection is basically a phase-difference detection it could be described by a single multiplication (alternatively, as a rectification process). Preliminary harmonic analysis of the response to sinusoidal stimuli, showed that the second harmonic is dominant while higher order harmonics contribute very little. Accordingly, the series of Eq. (1) was truncated after the quadratic term with small resulting error. The system memory was determined to be about 150 msec and consequently, the length of the identifying experiment was 40 sec in order to have a small (less than about 2%) statistical error in the kernel estimates.

A series of experiments was performed in which the standard deviation of the gaussian distribution of the excursion was varied. Such experiments were carried out for both the *Musca* and *Phaenicia* families of flies. This parametric variation was designed to reveal the spatial extent of correlation that gives rise to the detection of motion and whether the dynamic characteristics of the system of motion detection change with the spatial extent of the correlation process.

Fig. 2 shows the first order kernels, h_1, for different deviations of the moving pattern excursion for both the *Musca* and *Phaenicia* families. It is noted that the rise and response times as well as the waveforms are very similar indicating similar frequency response characteristics (this is upheld by the power spectra of Fig. 4a, b). The only prominent difference is in latencies; *Phaenicia* shows a latency of about 10 msec which remains constant with the degree of excursion while *Musca* has a shorter latency (about 5 msec) which varies with the deviation of the excursion. It is also noted, for both families, that the linear kernel (linear part of the system) increases initially with increases in the deviation of the moving stimulus but decreases for very large excursions. This is due to saturation of the unit response as it is also manifested by the power spectra shown in Fig. 4. It is further noted that for *Musca* h_1 attains a maximum for an excursion (standard deviation) of 4° while for *Phaenicia* the maximum occurs at 2° excursion. This correctly predicts and upholds the hypothesis that motion detection is due to correlation between adjacent

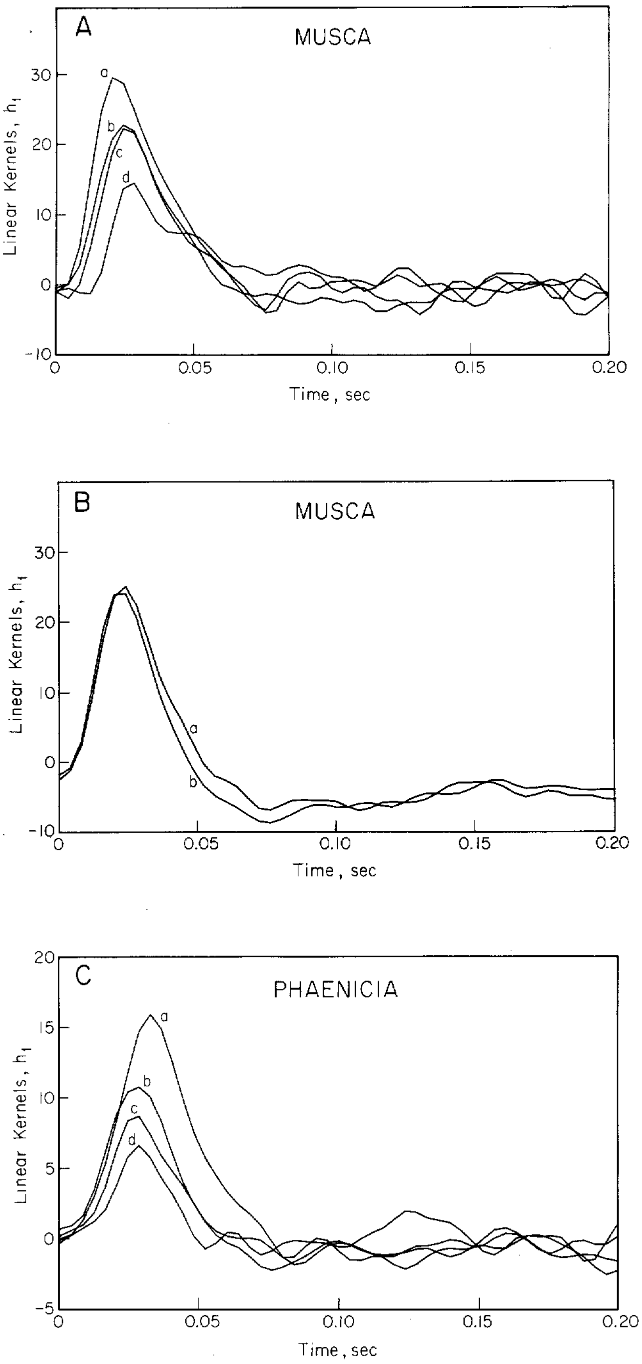

Fig. 2. First order kernels (h_1) derived from the moving striped pattern stimuli. The ordinate units are in (spikes/sec)/((light intensity unit) sec). a Linear kernels for *Musca*, for different standard deviations of the excursion of the gaussian white-noise input. The values for the different excursions are: *a* 4°, *b* 2°, *c* 1°, *d* 8°. b Two linear kernels (for *Musca*) derived from stimulating different portions of the unit field, one position being at the center of the field (curve *b*) and the other displaced 10° from the center (curve *a*). c Linear kernels for *Phaenicia* for different excursion deviations, *a* 2°, *b* 1°, *c* 1/2°, *d* 4°

Table I. Second order (nonlinear) kernels for the moving pattern studies (a) *Musca* (4° excursion deviation) (*b*) *Phaenicia* (2° excursion). The units of h_2 are (spikes/sec)/((intensity unit) · sec)^2

A) Musca, $h_2(\tau_1, \tau_2)$

τ_2, msec \ τ_1, msec	0	4	8	12	16	20	24	28	32	36	40	44	48	52	56	60	64	68	72	76	80	84	88
0	2																						
4	1	6																					
8	-2	6	17																				
12	-3	3	20	36																			
16	-2	-1	14	39	55																		
20	2	0	6	28	52	60																	
24	3	4	6	16	36	50	46																
28	3	3	8	15	23	34	34	23															
32	3	1	5	15	22	23	24	15	3														
36	0	-1	1	10	20	22	18	13	1	-10													
40	-3	-4	-3	4	14	20	18	12	7	-6	-15												
44	-1	-5	-6	-2	7	15	16	12	8	4	-7	-14											
48	5	-1	-7	-8	-2	8	14	12	6	4	3	-5	-9										
52	5	5	-2	-7	-9	-2	9	12	7	2	3	3	-2	-5									
56	2	5	3	-3	-7	-8	0	9	9	4	1	3	4	0	-3								
60	0	2	3	-2	-4	-4	-4	2	7	6	3	2	5	4	0	-1							
64	0	-1	-2	-3	-5	-4	-2	-1	2	4	4	3	3	6	4	0	0						
68	2	-1	-6	-8	-7	-6	-2	0	0	1	1	2	2	3	6	3	0	1					
72	4	1	-4	-11	-12	-8	-5	-1	1	2	-1	0	2	0	1	4	2	-1	1				
76	7	2	-1	-6	-14	-13	-7	-3	0	3	3	-1	0	2	-1	-1	3	0	-1	3			
80	6	6	0	-3	-8	-13	-11	-5	0	3	5	3	-1	1	3	0	1	3	-1	0	6		
84	0	5	3	-4	-6	-6	-9	-7	-1	3	5	6	3	0	2	5	2	3	3	-1	2	9	
88	0	-1	2	0	-6	-6	-4	-4	-2	2	5	6	6	4	0	3	6	3	3	2	-1	4	9

Table I-a

B) Phaenicia, $h_2(\tau_1, \tau_2)$

τ_2, msec \ τ_1, msec	0	4	8	12	16	20	24	28	32	36	40	44	48	52	56	60	64	68	72	76	80	84	88
0	3																						
4	-3	-2																					
8	-6	-4	-3																				
12	-3	-2	0	2																			
16	-1	1	5	10	14																		
20	-1	1	6	16	24	29																	
24	-1	0	3	10	27	38	41																
28	4	0	1	3	14	34	45	41															
32	11	5	2	3	6	17	36	40	29														
36	11	10	5	5	8	11	20	32	27	11													
40	2	10	8	3	8	14	16	19	25	12	-5												
44	-2	1	7	4	3	12	19	18	18	18	1	-16											
48	5	-1	-2	3	1	4	15	21	18	16	13	-6	-21										
52	7	7	-2	-6	-1	-1	6	17	19	15	15	11	-7	-18									
56	3	5	6	-3	-6	-3	1	10	18	15	11	15	12	-4	-10								
60	1	0	2	4	-2	-5	-2	6	16	19	11	8	14	11	1	-3							
64	-6	0	-3	1	4	-2	-3	4	12	19	19	9	5	10	8	1	-2						
68	-11	-7	-3	-3	2	3	-2	1	9	15	19	19	7	3	6	4	-1	-4					
72	-2	-9	-6	-2	-1	3	2	0	6	13	14	17	16	5	1	3	2	-3	-6				
76	8	-1	-6	-5	-3	-2	2	2	3	10	13	13	14	10	0	-2	3	1	-6	-7			
80	5	5	-1	-5	-5	-6	-5	0	2	5	9	11	12	12	5	-5	-4	2	-2	-7	-5		
84	-2	2	3	-2	-5	-5	-7	-6	-1	3	5	7	8	10	9	2	-6	-5	-1	-5	-5	2	
88	-1	-2	1	1	-3	-2	-1	-5	-5	1	6	5	4	6	7	7	3	-3	-4	-4	-5	1	10

Table I-b

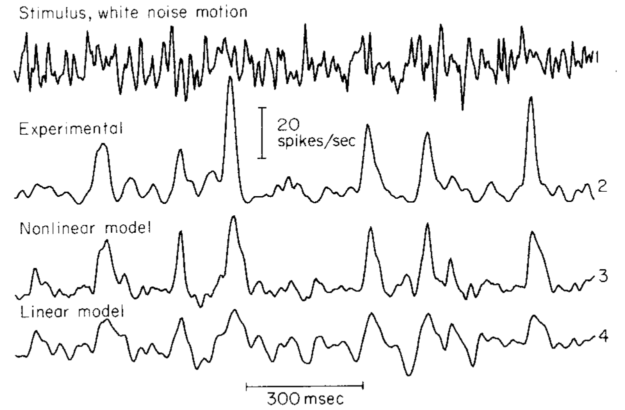

Fig. 3. Moving pattern studies: Model and experimental responses to the same portion of a white-noise input. The linear as well as the nonlinear model response are shown as they are computed from the derived model (kernel set $\{h_1, h_2\}$)

ommatidia. The figure also shows the h_1 resulting from a white-noise experiment in which the pattern was displaced so as to cover a different portion of unit field. No substantial change resulted in the derived model (h_1 and h_2). Table I describes the second order kernels of the motion detection system for both the *Musca* and *Phaenicia* families. As seen, the differences in the dynamic characteristics for the two families are minor (except for some difference in latency).

Fig. 3 shows the experimental response of the system to white-noise and the corresponding linear and nonlinear model responses. The agreement with experiment is very good for the nonlinear model.

The mean square error over the whole length of the record (40 sec) for the sequence of models, where the error for the zeroth order model, h_0, (a constant) is normalized to 100 units, is reduced as follows:

Model	Error
Constant $\{h_0\}$	100
Linear $\{h_1\}$	65
Nonlinear $\{h_1, h_2\}$	39

Therefore, the system exhibits, as expected, a considerable second order nonlinearity.

Fig. 4 shows the power spectra for experiment and model and for both families of flies. It is noted that the response level increases with the amplitude of the excursion but reaches a saturation level for excursion with standard deviation of about 8° for *Musca* and slightly higher for *Phaenicia*. The two families exhibit very similar frequency response characteristics as manifested by their response power spectra. They have a cutoff frequency at about 10 Hz which decreases somewhat as the excursion of motion increases.

The range of validity of the white-noise derived model is determined by certain experimental considerations. There are limitations imposed by the amplitude range of the stimulus, the stationarity of the system and several other factors (Marmarelis, 1972). One such limitation is the lower limit of the frequency range within which the model is valid. This is effectively determined by the length of time over which the experimental preparation can produce stationary response data and by the amount of computational power which is available. Usually the former is the determining factor. Since the white-noise experiments have to be repeated about 10 times, it was found that the maximum experimental stimulus-response record length is about 40 sec (i.e.

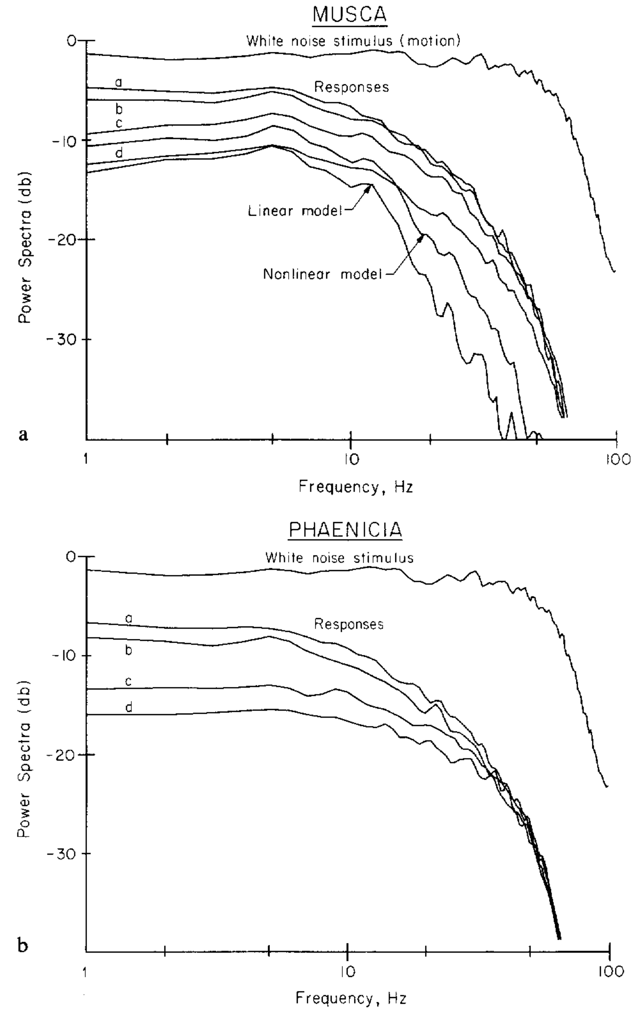

Fig. 4. Stimulus and response power spectra for the moving pattern studies. a *Musca a* 8°, *b* 4°, *c* 2°, *d* 1° excursions. Also shown are the spectra for the linear and nonlinear model responses for the 1° case. b *Phaenicia. a* 4°, *b* 2°, *c* 1°, *d* 1/2° excursions

about 400 sec or stable, stationary data). This being the case, the lower limit in the frequency band, for which the model is valid, is about 0.2 Hz. This derives from the fact that for a certain record length correlations can be computed reliably only up to about 1/10 to 1/20 of the record length. Therefore, in examining the model performance it is expected that the low frequency model predictions will be an extrapolation of the model performance at the lowest frequencies for which it is valid (i.e. about 0.2 Hz).

In view of these agreements between experimental results and model predictions (white-noise responses, power spectra) it is concluded that the white-noise derived model is an accurate description of the nonlinear dynamic transfer characteristics of this system.

The Two Spot Model. In these experiments the stimulus consisted of two spots of light placed with the line connecting them aligned with the axis of motion detection (Fig. 1) and properly spaced for maximum spatial correlation. The two lights (light "a" and light "b") were modulated by two independent white-noise sources. The power spectrum of this stimulus was flat from zero up to about 80 Hz. The distance between the two lights was two degrees for *Phaenicia* and four for *Musca*. These are the respective spacings producing maximum responses for two spot tests and they correspond to the facet spacings (McCann).

A nonlinear dynamic model was obtained for this two-input, one-output system by performing the analysis-synthesis process outlined earlier. Five characterizing kernels are thus obtained, $\{h_{1a}(\tau)$, $h_{1b}(\tau)$, $h_{2aa}(\tau_1, \tau_2)$, $h_{2bb}(\tau_1, \tau_2)$, $h_{2ab}(\tau_1, \tau_2)$ which, in essence, are the complete functional (nonlinear, dynamic)

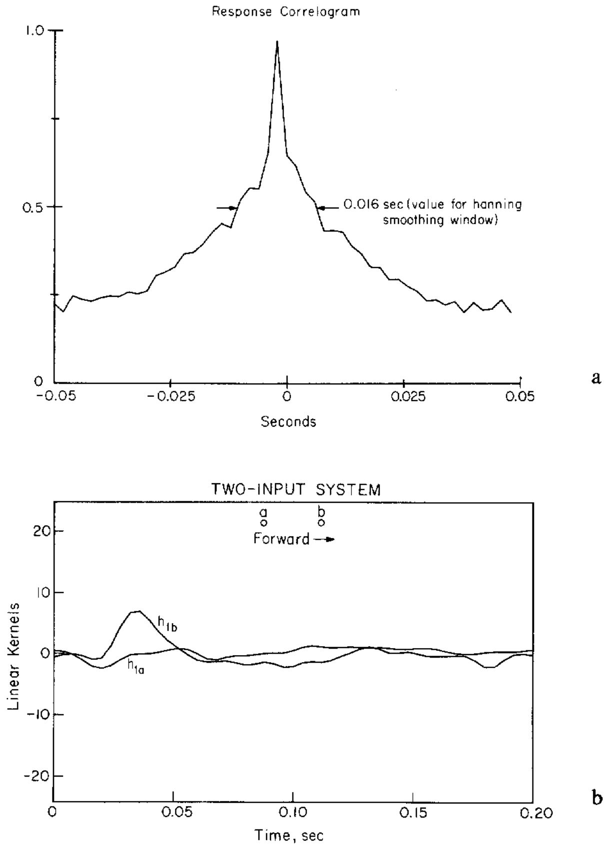

Fig. 5a. Crosscorrelogram of two experimental responses to the same white-noise stimulus of 40 sec duration. b The first order kernels $h_{1a}(\tau)$, $h_{1b}(\tau)$ for the two spot system (*Phaenicia*). The corresponding kernels for *Musca* are very similar. The ordinate units are (spikes/sec)/((intensity unit) · sec)

Table II. Second order kernels, $h_{2aa}(\tau_1, \tau_2)$, $h_{2bb}(\tau_1, \tau_2)$ and $h_{2ab}(\tau_1, \tau_2)$ for the two-input system. The units for the kernel are (spikes/sec)/((intensity unit) · sec)^2

$h_{2aa}(\tau_1, \tau_2)$

	τ_1, msec																						
τ_2, msec	0	4	8	12	16	20	24	28	32	36	40	44	48	52	56	60	64	68	72	76	80	84	88
0	1																						
4	0	2																					
8	0	3	5																				
12	-1	2	6	9																			
16	-2	-2	5	11	13																		
20	-1	-3	0	9	14	12																	
24	1	-2	-3	2	11	13	8																
28	3	-1	-3	-1	4	10	8	3															
32	4	0	-3	-1	2	4	7	5	1														
36	2	1	-3	-3	2	4	5	6	3	1													
40	0	1	-2	-4	-1	4	5	5	6	4	1												
44	1	0	0	-2	-2	1	4	4	5	5	3	0											
48	4	1	0	1	0	0	2	3	3	2	2	1	-3										
52	4	5	1	1	1	1	1	1	2	1	-1	-1	-1	-3									
56	2	4	4	1	0	1	1	2	1	2	0	-3	-2	-1	-1								
60	-1	1	3	2	1	0	1	3	3	2	2	-1	-3	-1	0	-1							
64	-3	-1	0	1	1	1	1	2	3	3	2	1	-2	-3	-1	-1	-2						
68	-1	-2	-2	-1	0	2	2	3	3	3	3	2	0	-3	-3	-2	-2	-3					
72	3	0	-2	-3	-2	1	2	3	3	1	3	5	2	-2	-3	-2	-2	-2	-2				
76	2	2	-1	-2	-4	-2	1	2	3	2	0	3	4	0	-2	-2	-2	-2	-1	-2			
80	-1	0	-1	-2	-2	-3	-1	2	3	3	1	-1	2	1	-2	-2	-2	-2	-1	0	0		
84	-1	-3	-4	-5	-3	-1	-1	1	3	4	3	1	-1	0	-1	-3	-2	-1	-1	0	0	0	
88	-1	-2	-4	-6	-8	-3	1	2	3	4	4	3	1	-1	0	-1	-3	-1	0	-1	-1	0	0
92	-1	-1	-1	-3	-7	-7	-2	2	4	4	4	4	3	1	-1	0	-1	-2	1	2	-1	0	1
96	-1	-2	-3	-1	-3	-5	-4	0	4	6	5	3	3	3	1	-1	0	0	-1	4	4	0	1
100	-2	-2	-4	-4	-2	-3	-3	-2	1	5	6	4	3	3	3	1	-1	0	1	1	6	5	-1
104	-2	-2	-3	-6	-5	-4	-4	-3	-2	1	5	5	3	2	3	2	1	0	2	2	2	6	4
108	0	-1	-2	-3	-5	-5	-4	-4	-3	-3	0	4	4	2	1	1	1	0	2	4	3	1	4
112	2	1	0	-1	-1	-3	-5	-4	-3	-2	-3	0	3	2	2	0	-1	0	1	3	5	2	0
116	1	3	2	1	0	0	-3	-4	-4	-1	-1	-3	0	2	3	2	0	-1	0	2	3	3	1
120	-4	1	4	3	1	0	-1	-3	-4	-3	0	-1	-4	-2	2	3	1	0	0	1	1	2	1
124	-3	-4	0	4	2	0	0	0	-2	-4	-2	0	-1	-4	-3	0	-1	-2	-1	1	0	0	2
128	1	-2	-5	0	3	1	0	1	2	0	-2	-2	1	-1	-4	-4	-3	-4	-3	-1	0	-1	0
132	2	3	-1	-5	1	3	-1	-1	2	3	2	0	-1	1	0	-3	-4	-5	-5	-3	-1	1	0
136	1	4	2	-3	-5	1	1	-2	-2	0	4	3	1	0	1	0	-3	-4	-3	-4	-3	-1	2
140	3	3	5	1	-5	-5	-1	0	-3	-4	-1	4	4	2	-1	0	-1	-5	-3	-1	-3	-4	-1

Table II-a

$h_{2bb}(\tau_1, \tau_2)$

	τ_1, msec																						
τ_2, msec	0	4	8	12	16	20	24	28	32	36	40	44	48	52	56	60	64	68	72	76	80	84	88
0	3																						
4	3	4																					
8	0	5	8																				
12	0	4	11	12																			
16	3	2	11	19	21																		
20	8	2	5	22	34	37																	
24	11	6	3	12	36	50	50																
28	7	11	6	4	19	47	60	55															
32	0	3	10	3	3	24	54	61	53														
36	3	-3	-1	5	-2	5	32	58	57	47													
40	1	4	-5	-7	-4	-4	13	43	59	50	38												
44	-4	1	3	-8	-14	-10	1	26	52	57	42	28											
48	-6	-4	0	0	-14	-19	-9	11	38	56	53	35	21										
52	-7	-7	-6	-6	-10	-21	-18	-3	20	43	52	44	28	17									
56	-8	-13	-10	-11	-16	-20	-21	-12	6	26	39	43	35	23	16								
60	-4	-13	-16	-14	-18	-25	-23	-14	-2	14	26	33	35	29	20	13							
64	-1	-6	-14	-18	-19	-27	-29	-18	-6	6	19	25	29	30	25	16	8						
68	-4	-2	-5	-13	-21	-24	-30	-27	-11	0	10	20	22	24	24	20	10	1					
72	-5	-4	-3	-5	-16	-25	-26	-29	-22	-5	4	12	19	19	17	17	13	1	-6				
76	0	-4	-4	-4	-10	-23	-27	-24	-25	-17	-1	7	14	19	14	11	12	6	-5	-6			
80	7	-2	-6	-7	-9	-19	-27	-25	-20	-20	-11	4	11	17	18	10	8	11	2	-5	-1		
84	7	4	-6	-12	-12	-15	-25	-26	-19	-13	-13	-5	8	14	17	15	7	6	9	1	-2	2	
88	-5	6	2	-10	-17	-16	-19	-26	-22	-11	-5	-5	1	11	13	14	13	5	4	8	0	-1	2
92	-9	-5	4	-1	-13	-21	-20	-21	-22	-15	-4	2	0	5	12	9	11	13	3	2	7	0	-1
96	-4	-9	-7	-1	-6	-16	-25	-22	-19	-17	-9	0	4	3	7	10	7	11	13	4	4	5	-2
100	0	-2	-8	-8	-5	-10	-20	-27	-21	-14	-10	-4	2	4	5	7	9	9	12	11	6	6	0
104	-3	2	1	-6	-9	-10	-14	-21	-24	-15	-7	-5	-1	3	4	5	6	9	10	12	8	7	4
108	-7	-4	3	2	-4	-9	-13	-15	-18	-18	-7	0	0	2	6	7	7	7	8	10	11	6	5
112	2	-10	-6	3	3	-4	-11	-16	-15	-14	-13	-1	5	2	4	9	9	8	8	7	9	8	3
116	7	2	-13	-8	2	5	-3	-14	-19	-15	-12	-11	1	6	4	8	11	8	8	8	4	5	4
120	-2	9	3	-12	-8	2	7	-4	-16	-18	-13	-12	-8	1	5	6	11	11	5	7	6	0	0
124	-5	1	11	4	-9	-9	0	4	-8	-16	-15	-11	-10	-6	1	4	4	9	9	4	7	4	-4
128	-3	-2	4	12	5	-8	-11	-5	-1	-10	-15	-12	-10	-8	-4	1	3	0	6	9	6	8	3
132	-1	0	1	6	12	4	-8	-12	-9	-5	-10	-14	-10	-7	-5	-3	4	3	-3	5	10	9	9
136	1	0	0	1	5	9	2	-7	-12	-10	-5	-10	-13	-6	-2	-2	-1	6	4	-3	6	11	9
140	-2	1	-1	-2	-2	2	4	0	-6	-12	-10	-4	-10	-12	-1	4	1	-2	5	5	0	8	11

Table II-b

Table II (continued)

	τ_1, msec																						
τ_2, msec	0	4	8	12	16	20	24	28	32	36	40	44	48	52	56	60	64	68	72	76	80	84	88
0	4	9	5	2	7	4	2	6	8	12	16	9	1	3	7	5	1	1	2	6	7	0	-7
4	-6	-1	7	6	6	11	7	5	7	6	8	12	5	-2	1	3	1	2	1	2	5	5	-3
8	-10	-12	-6	9	8	10	15	11	9	8	2	3	7	1	-3	-1	1	2	4	1	4	4	0
12	-10	-14	-16	-5	16	18	20	23	20	19	12	2	-1	5	-1	-4	3	7	6	2	2	5	-1
16	-2	-12	-18	-15	7	30	36	38	38	35	29	17	2	-2	5	-2	-3	8	12	5	-1	2	1
20	3	-6	-19	-24	-9	21	45	56	59	54	47	37	20	4	3	6	-4	-3	11	11	1	-2	2
24	1	-4	-20	-35	-33	-7	28	53	68	71	62	51	39	22	9	9	7	-6	-3	10	6	-1	0
28	-2	-6	-19	-42	-55	-42	-8	27	51	66	68	58	50	39	24	13	10	6	-5	-2	9	2	-1
32	-2	-9	-19	-37	-61	-68	-44	-7	25	45	56	55	49	47	38	22	11	9	7	-1	2	9	4
36	3	-8	-20	-34	-50	-69	-65	-36	-2	24	39	44	42	41	44	35	15	6	7	9	3	5	9
40	6	0	-16	-35	-49	-55	-61	-49	-24	0	20	32	33	32	35	35	26	10	3	5	7	3	6
44	4	4	-7	-28	-50	-58	-51	-44	-31	-16	0	16	27	25	23	25	22	16	8	0	2	4	1
48	5	4	-2	-20	-42	-59	-58	-44	-32	-18	-11	1	14	22	20	16	14	10	7	4	-2	0	2
52	4	6	0	-13	-32	-49	-58	-51	-40	-24	-12	-9	0	10	18	16	10	6	1	-1	-2	-4	-1
56	2	6	5	-6	-22	-38	-48	-49	-45	-36	-19	-9	-8	-4	4	13	9	4	-1	-7	-5	-3	-3
60	-1	2	5	-2	-14	-26	-36	-41	-40	-38	-29	-13	-7	-7	-6	1	9	5	0	-7	-10	-3	1
64	1	-3	0	-3	-13	-20	-27	-31	-31	-31	-29	-19	-9	-5	-5	-4	0	7	4	-3	-9	-6	4
68	5	0	-2	-1	-10	-20	-23	-25	-24	-24	-24	-20	-14	-7	-2	0	-3	-2	6	4	-4	-7	-1
72	4	6	3	1	-1	-12	-22	-23	-21	-18	-17	-17	-16	-13	-4	4	7	-3	-5	4	2	-3	-7
76	1	6	10	5	1	-3	-15	-25	-24	-18	-15	-12	-12	-13	-11	2	13	13	-4	-10	1	2	-2
80	0	1	7	10	3	-2	-7	-21	-29	-23	-18	-16	-7	-8	-12	-9	6	18	15	-6	-14	-2	4
84	7	-4	-2	6	8	1	-4	-10	-23	-26	-19	-17	-12	-3	-5	-10	-8	6	19	15	-7	-13	-4
88	0	4	-7	-4	3	5	1	-4	-10	-19	-18	-13	-13	-8	0	-3	-8	-7	7	19	16	-2	-8
92	-7	2	4	-5	-5	-1	1	-3	-9	-11	-14	-13	-10	-10	-6	0	0	-3	-3	8	17	19	7
96	4	-3	6	8	-2	-5	-4	-5	-13	-15	-12	-12	-11	-9	-10	-6	2	4	-1	-1	7	13	20
100	3	4	1	11	13	3	-5	-9	-13	-19	-16	-11	-9	-7	-6	-8	-4	4	3	0	2	4	10
104	-8	2	2	4	13	13	2	-8	-13	-17	-19	-13	-9	-4	2	-1	-4	-2	3	2	2	5	3
108	-10	-4	1	0	5	12	10	-2	-11	-16	-15	-13	-11	-11	-1	7	4	0	-1	2	4	7	7
112	-9	-6	2	3	1	6	10	5	-5	-12	-13	-10	-8	-12	-14	-2	6	6	1	-2	2	6	9
116	-7	-8	-1	8	7	3	5	8	4	-3	-10	-10	-7	-7	-12	-13	-4	2	5	-1	-6	-1	2
120	7	-8	-7	3	11	10	5	6	7	1	-4	-11	-11	-6	-7	-10	-9	-5	-2	3	-4	-9	-6
124	10	7	-5	-3	4	12	11	7	9	6	-2	-6	-13	-11	-6	-6	-7	-7	-8	-5	2	-4	-10
128	-4	8	8	2	0	3	11	9	6	11	6	-1	-7	-12	-11	-5	-5	-6	-8	-11	-5	2	-4
132	-11	-8	4	7	5	2	2	6	3	4	10	6	2	-6	-12	-10	-5	-4	-5	-8	-10	-4	0
136	-12	-12	-7	2	6	5	0	-2	-1	-3	0	6	4	-1	-9	-12	-7	-5	-4	-4	-7	-8	-4
140	-10	-13	-9	-1	2	3	2	-3	-4	-7	-8	-4	1	0	-7	-13	-10	-4	-7	-6	-4	-6	-7

CROSS-KERNEL $h_{2ab}(\tau_1, \tau_2)$

Table II-c

model of the system. The set $\{h_{1a}(\tau), h_{2aa}(\tau_1, \tau_2)\}$ are called the self-kernels due to input "a" and describe the contribution of this input to the total system response. Similarly for set $\{h_{1b}(\tau), h_{2bb}(\tau_1, \tau_2)\}$. Kernel $h_{2ab}(\tau_1, \tau_2)$ is the cross-kernel (or interaction kernel) and denotes the nonlinear interaction of the two inputs as it affects the system response (Fig. 8 see page 84).

Fig. 5 shows the two first order kernels h_{1a} and h_{1b}. It is to be noted that they are different. They are the impulse response set of functions which is the best linear model (in the mean-square sense) of the physical system. $h_{1b}(\tau)$ is positive while $h_{1a}(\tau)$ is somewhat negative. This is a manifestation of selectivity; if an impulse is given at input "b" a positive reaction (increase from the mean response level) will be evoked while an impulse given at "a" will elicit a negative reaction (decrease of the mean response). In interpreting these results it should be noted that the two inputs at "a" and "b" have a certain steady light (d.c. value) and the input signals are measured with respect to this level taken as reference (zero level). Table II shows the two self-kernels h_{2aa} and h_{2bb}. Similar comments apply to them; self-kernel h_{2aa} is very small (nearly null) while self-kernel h_{2bb} is large and positive. This is again a manifestation of selectivity. The contribution of these self-kernels to the system response can be seen in Figs. 6 and 7. It should be noted that while the self-kernels describe the contribution of each input separately, their determination is dependent on the fact that there is a nonzero, steady (d.c.) signal at the other input. Thus, in a sense, they can also be interpreted as correlating two input signals. For example, they describe the (nonlinear) "on-off" characteristics (Fig. 11b) and the double harmonic in the response (Fig. 15b).

Table II shows the interaction kernel $h_{2ab}(\tau_1, \tau_2)$. It is here that the "selectivity in motion detection" is clearly exhibited. In the region $\tau_1 > \tau_2$ there is a large positive peak (forward motion) while in the region $\tau_2 > \tau_1$ there is a large negative peak (reverse motion). As described earlier, this kernel denotes quantitatively the contribution to the response which is due to the nonlinear dynamic interaction between the input at "a" and the input at "b". Times τ_1 and τ_2 denote the occurrence in the past of stimuli at input "a" and input "b" respectively. Therefore, it is expected that a pulse at "a" followed by a pulse at "b" (i.e. $\tau_1 > \tau_2$) will elicit a large positive response while a pulse at "b" followed by a pulse at "a" (i.e. $\tau_2 > \tau_1$) will produce a negative response. These expectations are upheld by h_{2ab} as these two cases are evidenced by the positive and negative peaks. Moreover, h_{2ab} clearly shows the temporal extent of such "crosstalk" (about 60 msec) as well as what the time history of the elicited response would be. In essence, h_{2ab} is a complete nonlinear dynamic description of the selective part in the response of the Class II unit, as evoked by the two spot stimuli.

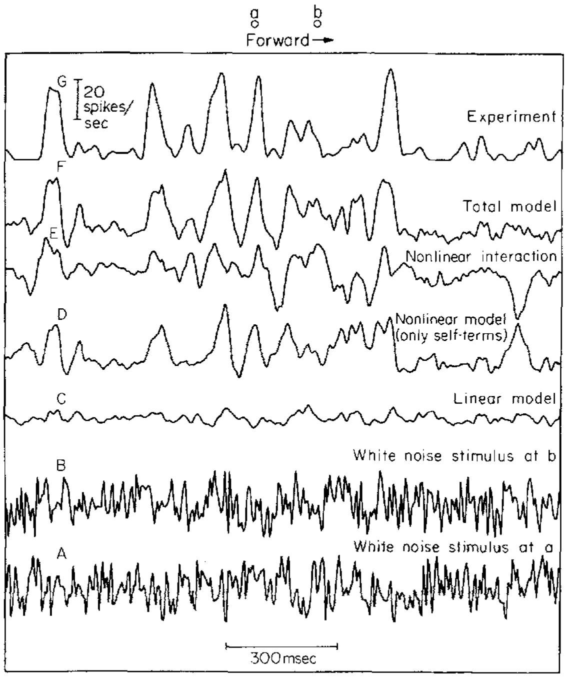

Fig. 6. Experimental and model responses to the same white-noise stimuli for the two input system (*Phaenicia*). A: A portion of the white-noise stimulus (light intensity fluctuating in time) at spot "a", B: white-noise stimulus at spot "b", C: evoked model response to stimuli at "a" and "b" due to linear terms (h_{1a} and h_{1b}), D: model response due to kernels h_{1a}, h_{2aa}, h_{1b}, h_{2bb}, E: model response due to interaction kernel h_{2ab}, F: total model response and G: corresponding experimental response

Fig. 6 shows the white-noise stimuli as well as the experimental and model-derived responses to a portion of the white-noise signals used in the identifying experiment. The model responses have been broken up into the different components. The mean square error reduction, where the error for the $\{h_0\}$ model (i.e. a constant equal to the average response) is 100 units, is as follows:

Model		Error
Constant	$\{h_0\}$	100
Linear	$\{h_{1a}, h_{1b}\}$	97
Self-, nonlinear	$\{h_{1a}, h_{1b}, h_{2aa}, h_{2bb}\}$	69
Total, nonlinear	$\{h_{1a}, h_{1b}, h_{2aa}, h_{2bb}, h_{2ab}\}$	38

It is noted that the system is strongly nonlinear (the linear model produces only a 3% reduction of the error) and that the nonlinear dynamic cross-talk (between "a" and "b") term is very large (31% error reduction from the self-kernel model).

Fig. 7 shows the response power spectra for both experiment and model as well as the spectra of the two white-noise stimuli. The white-noise stimuli have a flat power spectrum from essentially d.c. up to about 80 Hz. The system has a cutoff frequency of about 5 Hz and rolls off at very high frequencies at a rate of 24 db/octave. It should be noted that the model

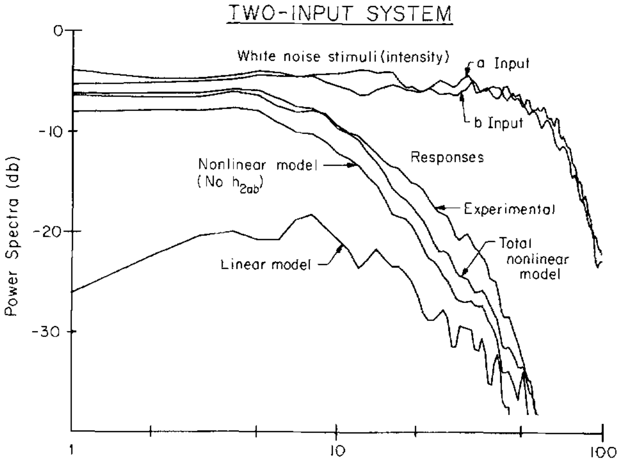

Fig. 7. Power spectra of white-noise stimuli and corresponding experimental and model responses for the two-input system

performance at high frequencies (above 20 Hz approximately) deviates somewhat from the experimental response. This is due to the smoothing of the response function, as described earlier, and the fact that the model has been computed only up to the second harmonic (it should be noted how the addition of the second order nonlinearity improves the high frequency model performance in Fig. 4 and Fig. 7).

V. Analysis of Nonlinear Models; Derivation of Moving Pattern Model from Two Spot Models

Two nonlinear dynamic models of the Class II unit system are presented. In one case the whole field of the unit was used and the stimulus consisted of a striped pattern moving randomly in white-noise fashion and in the other case the "fundamental unit" of the field was tested with two closely spaced spots. An interesting example of the power of such models in generalizing the results is provided by a calculation of the motion model kernels from those of the two spot model. Two questions arise: (*a*) are the two models compatible? (*b*) does comparison of the two models suggest the manner in which the "small field" contributions as manifested by the two-adjacent-ommatidia system add up to produce the large field response? To answer these two questions the hypothesis is made that the large field response is due to a linear (weighted) summation of all the two-adjacent ommatidia systems. The consequences of this assumption are examined to verify or dispute the hypothesis, as it would be revealed by the sets of kernels derived in the two cases.

Regarding the one-input system the stimuli induced in the corresponding two-ommatidia system are considered. The induced input at "a" is $s(t)$ while the input at "b" is $s(t-\alpha)$ where α is the transport delay in moving from "a" to "b". In the case that the stimulus is a pattern moving in white-noise fashion, α is a gaussian random variable. It is also taken, to a good approximation, that the induced flux at input "a" or "b" is gaussian white-noise. Then the linear part of the model is

$$E\left\{\sum_F \left[\int h_{1b}(\tau)\, s(t-\alpha-\tau)\, d\tau + \int h_{1a}(\tau)\, s(t-\tau)\, d\tau\right]\right\}$$

(E denotes "expected value" and $\sum\limits_F$ denotes summation over field F) which after a simple change of variable becomes

$$E\left\{\sum_F \int [h_{1a}(v) + h_{1b}(v-\alpha)]\, s(t-v)\, dv\right\}$$

Therefore the relationship that must be obeyed between the first order kernels, $\{h_{1a}, h_{1b}\}$, of the two-input case and the single first order kernel, h_1, of the one-input case, is

$$h_1(v) = E\{h_{1a}(v) + h_{1b}(v-\alpha)\} \tag{6}$$

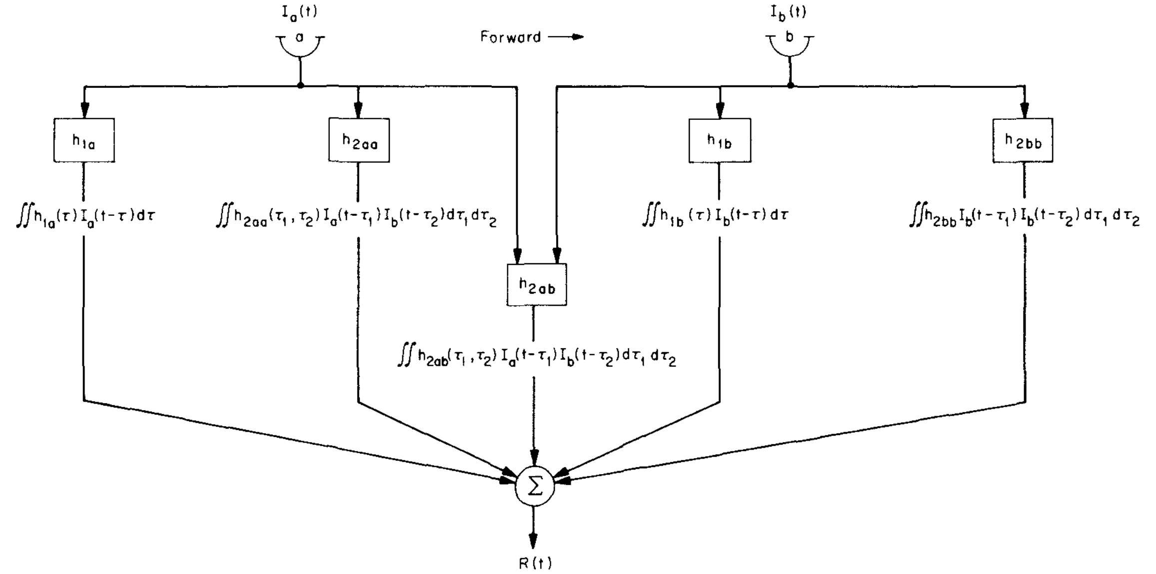

Fig. 8. Block diagram of derived model for two-input system showing the contribution due to each kernel

since the summation is linear and all h_{1a}'s and h_{1b}'s are identical. Similarly, considering the second order (nonlinear) self term h_{2bb}, produces the term

$$\iint h_{2bb}(\tau_1, \tau_2)\, x(t-\alpha-\tau_1)\, x(t-\alpha-\tau_2)\, d\tau_1\, d\tau_2$$

which after a simple change of variable becomes

$$\iint h_{2bb}(v_1-\alpha, v_2-\alpha)\, x(t-v_1)\, x(t-v_2)\, dv_1\, dv_2\,.$$

Similarly, for the term corresponding to kernel $h_{2aa}(\tau_1, \tau_2)$. The "cross-talk" term becomes

$$\iint h_{2ab}(v_1, v_2-\alpha)\, x(t-v_1)\, x(t-v_2)\, dv_1\, dv_2$$

which is symmetricized by taking

$$h^*_{2ab}(v_1, v_2, \alpha) = \tfrac{1}{2}\left[h_{2ab}(v_1, v_2-\alpha) + h_{2ab}(v_2-\alpha, v_1)\right].$$

Then, the relationship that must be obeyed between the second order kernels of the two systems is

$$h_2(v_1, v_2) = E\left[h_{2aa}(v_1, v_2) + h_{2bb}(v_1-\alpha, v_2-\alpha) + h^*_{2ab}(v_1, v_2, \alpha)\right]. \quad (7)$$

Computer calculations produced the kernels of Fig. 9 which are compared to those obtained directly from the motion stimulus. This shows that the two models are essentially the same except for the greater response latency of the model derived from the two spot stimulus. Previous tests of these units have shown that as the area of a stimulus increases the latency decreases when compared to stimuli of the same intensity per unit area which explains the added latency in Fig. 9.

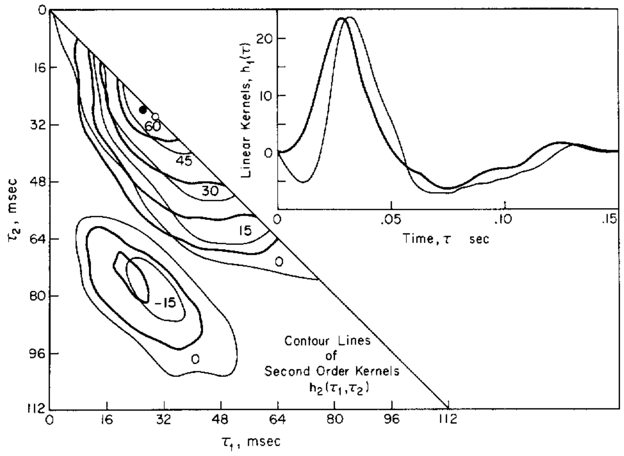

Fig. 9. Comparison of kernels, $h_1(\tau)$ and $h_2(\tau_1, \tau_2)$ for moving pattern system (heavy lines) and equivalent system derived from the two-spot system (light lines). The second order kernels are shown in terms of equal-altitude contours

Comparison of Moving Pattern Model Predictions and Experimental results. This type of stimulus has been used extensively for insect vision research. Responses to sinusoidal pattern oscillations and suddenly applied motion are compared for a range of frequencies. The model responses conform quite precisely to direct experimental tests in this case for frequencies from 0.2 to 50 Hz. It will be noted from Fig. 10a that the first order terms of the model

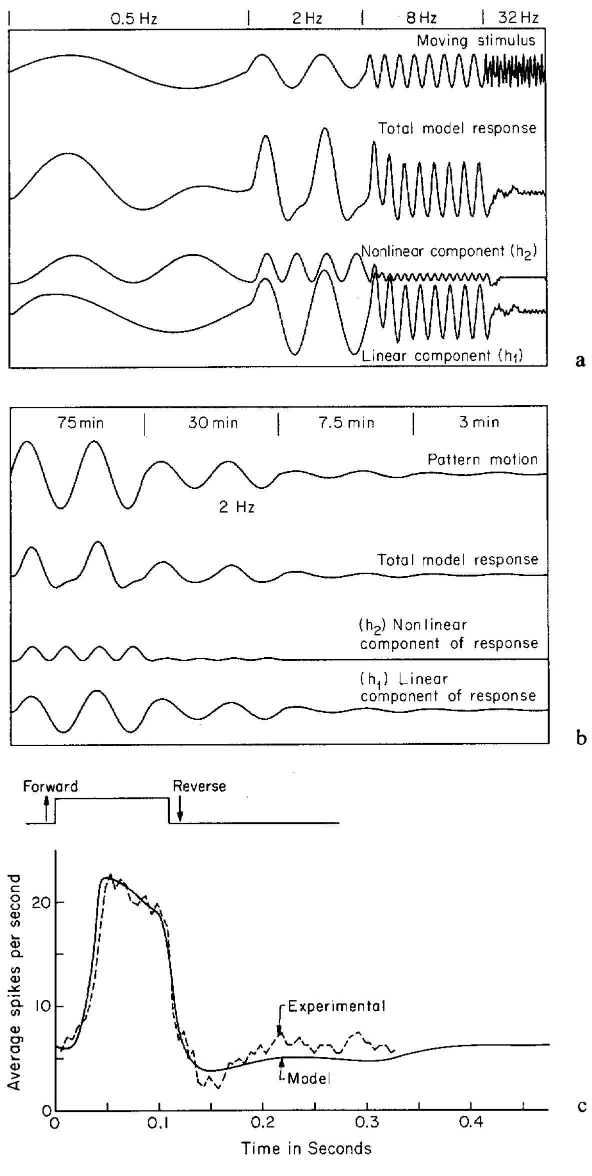

Fig. 10. Responses of moving pattern system. *Musca* Class II unit. a Model derived sinusoidal responses for different frequencies. The linear (due to h_1) and nonlinear (due to h_2) components are shown. b Model responses to a sinusoidal stimulus of decreasing amplitude. c Model and experimental responses to a pulse stimulus producing both "forward" and "reverse" jumps of 1 degree

produce the dominant response contribution and that the second order term produces a second harmonic in the response that attenuates more rapidly with frequency than the fundamental. All of these properties conform accurately to the results of direct experiments.

Previous tests had been conducted to determine the response threshold for this same type of pattern in terms of the amplitude of oscillation (McCann and Foster, 1971). These showed that a detectable response could be measured for amplitudes as low as 5 minutes of an arc of zero-to-peak amplitude at a frequency of 2 Hz. Model calculations pertinent to this are presented in Fig. 10b indicating detectable responses down to and below 3 minutes. Absolute thresholds of this sort are a complex function of the test conditions and the nature of the noise in the response. However it is to be noted that greater sensitivity is to be expected from the model because the determination of the characterizing kernels by cross-correlation techniques is affected less by the presence of noise than averaged responses from a series of repeated stimuli (Marmarelis, 1972). A critical test for the high frequency range of the model is to present a sudden displacement in a very short time interval. Model and direct experimental data for this are shown in Fig. 10c. The agreement between the two is seen to be very good.

The Two Spot Model. Comparisons of predicted model responses to the specific tests (McCann) are presented in Figs. 11 through 14. As indicated by this sample all previous tests (McCann) were accurately duplicated by the model within its prediction ranges of intensity and frequencies. The only significant differences are for very low frequencies which are below the frequency range of the model (about 0.2–50 Hz) and for mean intensity conditions that differ significantly from the mean intensity for which the model is valid (midway between response threshold and saturation). The dominant model kernels are h_{2bb} and h_{2ab}. The response component due to h_{2bb} is a function of the intensity I_b alone and its time history over the time span (system memory) for which it affects the system response.

Typical step experiments to approximate forward and reverse motion are illustrated in Fig. 11. In Fig. 11a such forward and reverse sequences are compared to actual tests made on a different preparation than the one used for the kernel calculations. In Fig. 11b the total model responses are compared to those in which the cross-kernel h_{2ab} is excluded from the model. This illustrates the relative roles of the two dominant terms h_{2bb} and h_{2ab} in different typical switching sequences (McCann).

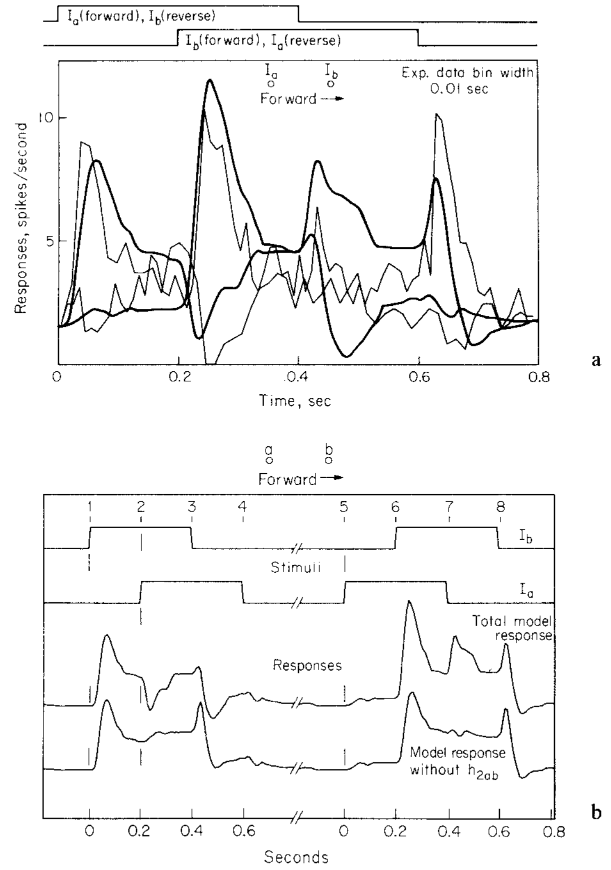

Fig. 11. Experimental and model predicted responses to pulse stimuli at inputs "a" and "b". No background, initial intensities as specified for white noise tests. Intensity change is 40% of initial values. a The heavy lines show the model response and the light lines show the experimental response. The experimental data were obtained from a different preparation than the one which was used in the identifying experiment. b Model predicted responses to pulse stimuli showing both the total response and the response resulting by excluding the term due to $h_{2ab}(\tau_1, \tau_2)$

The experimental data of Fig. 11a show good agreement with the model. The experimental responses do not, however, give a good representation for the wave shape details. As previously described (McCann) to obtain the response wave shape accurately by direct tests hundreds of repeated experiments are required as well as smoothing procedures to remove the high frequency noise (both naturally occurring and artificially introduced through histogramming). These difficulties are more effectively treated in the white noise model. Such a direct test (McCann, Fig. 6b) confirms the wave shape of the transients of Fig. 13 with a rise time of about 0.05 sec showing that the upper frequency range of the model is adequate. However, Figs. 11a, b show an additional variation in the details of the individual transient responses. Referring to Fig. 11b, it is seen that the third transient in the sequence of responses is determined almost completely by the cross term h_{2ab} which produces a somewhat different wave shape than that due to h_{2bb}.

Fig. 13a shows the model prediction for the critical tests of McCann (Fig. 6b) that illustrated the relative roles of ΔI_a, ΔI_b changes in simulating forward motion. The correspondence is precise except for the rise time to peak of one case (curve 3).

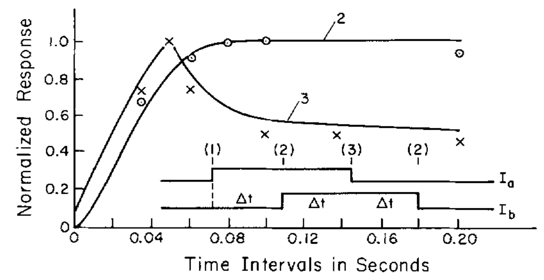

Fig. 12. Two-input system: Magnitude of transient response as a function of the time interval Δt for two different stimulus conditions

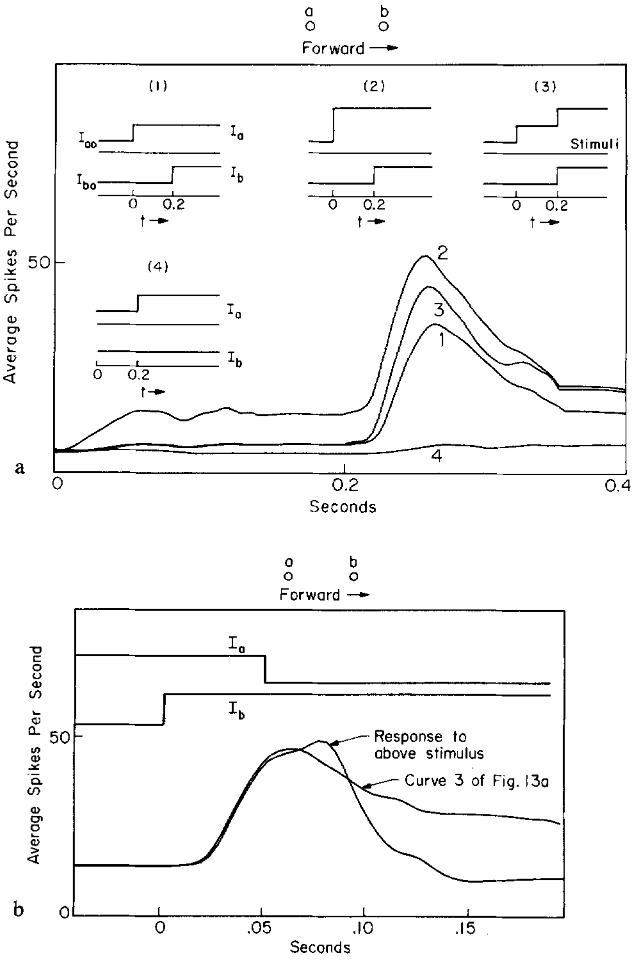

Fig. 13. Model derived response for additional pulse stimuli used previously (McCann). a Correspond to McCann (Fig. 6b); b Stimulus corresponding to group 3, Fig. 12

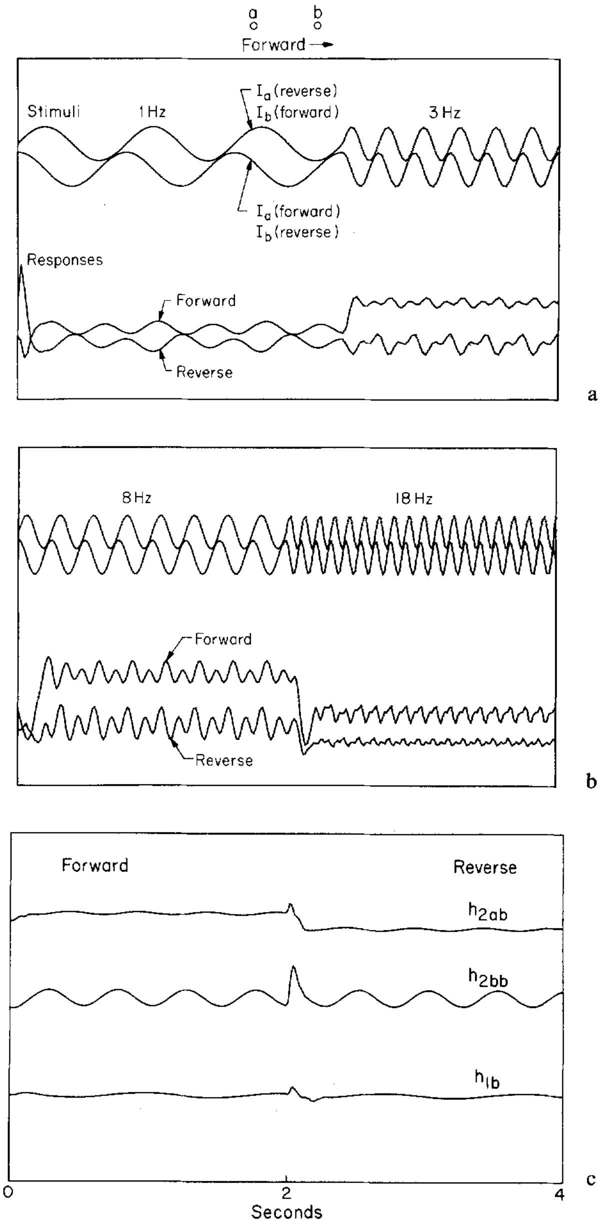

Fig. 14. Model responses to sinusoidal stimuli for the two-input system. a and b Both forward I_a leads I_b by 90°) and reverse I_b leads I_a by 90°) conditions and the evoked responses for different frequencies. c Model response components for both forward and reverse motion for a stimulus of 1 Hz. Total response shown in Fig. 14a

The previous study (McCann) indicated three general groups of characteristic transients; one of these consisted of changes in only one input (spot), the second consisted of sequential changes in both inputs in the same direction and the third consisted of changes in opposite directions. Fig. 11 illustrates examples of all these groups and shows that the response terms due to h_{2bb} and h_{2ab} combine in a variety of ways to produce the different total responses.

One indication of a difference between group 2 and 3 responses was obtained by determining the change in the integral of the difference between paired forward-reverse responses with changes in the switching interval (Δt) (McCann). Fig. 12 shows the comparison of these previous tests to the model predictions for intervals up to 0.2 seconds (the reliable range of the model).

The peak at about 0.05 sec for curve 3 (Fig. 12) is caused by the characteristics shown in Fig. 13b for the condition of sequential changes in opposite directions that cause transients of opposite polarities whose sum peaks at this time.

Responses to sinusoidal intensity variations are illustrated in Fig. 14. It is noted that a strong second harmonic is exhibited in the response. This is shown by Fig. 14c to come primarily from the h_{2bb} term while the steady selective response is due to h_{2ab}. The selectivity in motion detection as manifested by the difference between "forward" and "reverse" response levels is seen to attain a maximum for frequencies between 3–8 Hz. The superior method of dealing with the problem of low signal-to-noise ratio is shown by a comparison of these model responses and the direct tests (McCann, Fig. 12). The second harmonic components of responses (McCann, Fig. 12b) are actually computed from the model.

VI. Summary and Discussion

The first purpose of this paper was to develop and evaluate a suitable nonlinear system identification method for studying visual nervous systems. The extension of white-noise theory presented here provides a basis for both multiple-input, multiple-response experiments and the representation of a spatial parameter as an added independent variable in defining visual pattern recognition functions. Specifically illustrated is the case of two finite difference spatial elements and the extension to more complex spatial variations is straightforward.

The importance of preliminary tests and analyses (some of them on the same preparation used for computing the model kernels) must be emphasized. The most critical are (1) preliminary response power spectra analysis as a function of the stimulus power spectra to optimize the stimulus spectral range, (2) tests to determine the system memory in order to determine the length of the identification experiment (3) cross-correlations of successive sets of responses to identical white-noise stimuli in order to determine the signal-to-noise ratio of the specific preparation which gives an indication of the system stationarity and determines the smoothing window in processing the stimulus-response data in order to reduce the noise content and (4) harmonic analysis of the response to representative single frequency tests over the system bandwidth to determine the required number and order of kernels in the model for a given accuracy.

The need for limitation in the range of temporal and spatial frequencies and the intensity in the stimuli requires a preliminary knowledge of the general response properties. For this study the temporal frequency was limited to 0.2–50 Hz and the initial reference level of the intensity was half way between the response threshold and saturation with a dynamic range of variation of 1.6 log units. As shown by the above examples, the accuracy of prediction of the derived models in comparison to the previous discrete tests (McCann) was extremely good for this range of conditions. Most differences were attributable to inaccuracies in the discrete results due to an inferior method of handling the noise problem inherent in the discrete tests. A generalization of the model requires both the development of adequate test procedures to study the longer time constants (adaptation) of the system and additional white-noise tests at other mean spot intensities in order to cover the whole operational range of the system.

The second purpose of the study was to provide a nonlinear dynamic model of the basic motion detection process in flies. This model represents a quantitative and concise definition of the system from which principles of pattern recognition can be deduced and functional characteristics relevant to neural physiology can be obtained. The results in these areas are quite rich but cannot be covered in this same paper since they require correlation with similar white-noise studies of the more complete system, particularly with the "ON" fibers (Arnett) and the retinula cells. They also require correlation with morphological studies to be reported separately.

A few points relevant to the specific properties of a pattern's motion that causes the selective responses of these units should be emphasized. In this connection it must be realized that the five kernels of the two spot model were determined for a fixed initial (average) intensity of both spots (i.e. a certain fixed adaptation level). All five kernels show a form of motion selectivity. The terms $\{h_{1b}, h_{2bb}\}$ give positive responses for changes in the trailing spot intensity (I_b) while $\{h_{1a}, h_{1aa}\}$ give small negative responses for variations in the spot intensity I_a) which is the trailing spot for reverse motion. It is only the cross-kernel h_{2ab} that correlates the rates of changes of both intensities and the time histories of their relative values and produces the large inhibition responses for reverse motion. It is thus to be expected that for a moving pattern of recurrent form (such as with a single spatial wavelength) this latter term would produce the dominant contribution of the directionally selective response. This fact is illustrated by Fig. 14c where it is seen to produce the difference in the steady (d.c.) terms of the selective responses. For a nonrepeating pattern in forward motion the major contribution to the selective response comes from term h_{2bb} (Fig. 11).

The large field Class II units specifically used here to develop the models have been shown to algebraically sum to a good approximation the small field contributions as defined by the two spot model. The minor deviations from this rule are attributable to the large initial response latency of the Class II units to small field stimuli as compared to large field ones. This shows up in the comparison curves of Fig. 9 in two ways. One is the small relative displacement of the resulting kernel functions and the other is the slight broadening of the wave form of the derived model functions as compared to those derived from the direct motion tests.

The principal pattern recognition function of the large field Class II units has been postulated to be the determination of the gross or average motion in the total field relative to the insect's motion (McCann and Foster, 1972). Both models show that the Class II unit responses are greater when all elements of the total field have the same direction of motion. If this total field motion is that of a simple recurrent pattern the h_{2ab} term of the two spot model provides the principal contribution to the total field response. If it is nonrecurrent the h_{2bb} term dominates the evoked response for the forward motion condition. The ability to derive the large field pattern motion model from the small field two spot model illustrates an effective method of combining the results of groups of white-noise experiments in order to develop a more comprehensive model.

The previous study (McCann) showed a fundamental difference in spot transient switching combinations approximating continuous intensity variations which were described as group 2 when the spots changed in the same directions and group 3 when the changes were in opposite directions. These can be related to the relative contributions of the kernels. As illustrated by Figs. 11 and 13, simulation of forward motion in group 2 is initiated by ΔI_b (the trailing spot) and both h_{2bb} and h_{2ab} contribute to the resulting stimulus transients – whereas in group 3 the stimulus is initiated by ΔI_a and only h_{2ab} makes a significant contribution. For reverse motion simulations the inhibition transients for both group 2 and group 3 as initiated by ΔI_a and ΔI_b respectively are due principally to h_{2ab}.

Acknowledgements. This research was supported by the National Institutes of Health, U.S. Public Health Service grants GM 15537 and NS 03627.

References

Arnett, D. W.: Receptive field organization of units in the first optic ganglion of diptera. Science **173**, 929–931 (1971).

Bishop, L. G., Keehn, D. G., McCann, G. D.: Motion detection by interneurons of optic lobes and brain of the flies *Calliphora phaenicia* and *Musca domestica*. J. Neurophysiol. **31**, 509–525 (1968).

Lee, Y. W., Schetzen, M.: Measurement of the kernels of a nonlinear system by cross-correlation. Quart. Prog. Rept. No. 60, Research Lab. of Electronics, M.I.T. 1961.

Marmarelis, P. Z.: Nonlinear dynamic transfer functions for certain retinal neuronal systems. Doctoral Thesis, California Institute of Technology 1971.

Marmarelis, P. Z., Naka, K.-I.: White-noise analysis of a neuron chain: An application of the Wiener theory. Science **175**, 1276–1278 (1972).

Marmarelis, P. Z.: Nonlinear identification of bioneuronal systems through white-noise stimulation. Thirteenth Joint Aut. Control Conf., 117–126, Stanford University 1972.

McCann, G. D., MacGinitie, G. F.: Optomotor response studies of insect vision. Proc. Roy. Soc. B. **163**, 369–401 (1965).

McCann, G. D., Dill, J. C.: Fundamental properties of intensity, form and motion perception in the visual nervous systems of *Calliphora phaenicia* and *Musca domestica*. J. Gen. Physiol. **53**, 385–413 (1969).

McCann, G. D., Foster, S. F.: Binocular interactions of motion detection fibers in the optic lobes of flies. Kybernetik **8**, 193–203 (1971).

McCann, G. D., Arnett, D. W.: Spectral and polarization sensitivity of the dipteran visual system. J. Gen. Physiol. **59**, 534–558 (1972).

McCann, G. D., Foster, S. F.: Light adaptation for visual pattern recognition in flies. Vision Research (in press).

McCann, G. D.: The fundamental mechanism of motion detection in the insect visual system. Kybernetik **12**, 64–73 (1973).

Wiener, N.: Nonlinear problems in random theory. New York: Wiley 1958.

P. Z. Marmarelis
G. D. McCann
California Institute of Technology
Pasadena, California 91109, USA